Functional and histopathological improvement of the post-infarcted rat heart upon myoblast cell grafting and relaxin therapy

Massimo Bonacchi [a, †], Silvia Nistri [b, †], Cristina Nanni [c], Sandro Gelsomino [d], Alessandro Pini [b], Lorenzo Cinci [b], Massimo Maiani [a], Sandra Zecchi-Orlandini [b], Roberto Lorusso [d], Stefano Fanti [c], Josh Silvertown [e], Daniele Bani [b, *]

[a] *Department of Medical and Surgical Critical Area, Cardiac Surgery Unit, University of Florence, Florence, Italy*
[b] *Department of Anatomy, Histology & Forensic Medicine, University of Florence, Florence, Italy*
[c] *Nuclear Medicine Unit, S.Orsola-Malpighi Hospital, Bologna, Italy*
[d] *Experimental Surgery Unit, Careggi Hospital, Florence, Italy*
[e] *Ontario Cancer Institute, University Health Network, Toronto, Canada*

Received: June 18, 2008; Accepted: September 7, 2008

Abstract

Although the myocardium contains progenitor cells potentially capable of regenerating tissue upon lethal ischaemic injury, their actual role in post-infarction heart healing is negligible. Therefore, transplantation of extra-cardiac stem cells is a promising therapeutic approach for post-infarction heart dysfunction. Paracrine cardiotropic factors released by the grafted cells, such as the cardiotropic hormone relaxin (RLX), may beneficially influence remodelling of recipient hearts. The current study was designed to address whether grafting of mouse C2C12 myoblasts, genetically engineered to express green fluorescent protein (C2C12/GFP) or GFP and RLX (C2C12/RLX), are capable of improving long-term heart remodelling in a rat model of surgically induced chronic myocardial infarction. One month after myocardial infarction, rats were treated with either culture medium (controls), or C2C12/GFP cells, or C2C12/RLX cells plus exogenous RLX, or exogenous RLX alone. The therapeutic effects were monitored for 2 further months. Cell transplantation and exogenous RLX improved the main echocardiographic parameters of cardiac function, increased myocardial viability (assessed by positron emission tomography), decreased cardiac sclerosis and myocardial cell apoptosis and increased microvascular density in the post-infarction scar tissue. These effects were maximal upon treatment with C2C12/RLX plus exogenous RLX. These functional and histopathological findings provide further experimental evidence that myoblast cell grafting can improve myocardial performance and survival during post-infarction heart remodelling and dysfunction. Further, this study provides a proof-of-principle to the novel concept that genetically engineered grafted cells can be effectively employed as cell-based vehicles for the local delivery of therapeutic cardiotropic substances, such as RLX, capable of improving adverse heart remodelling.

Keywords: myocardial infarction • heart remodelling • relaxin • C2C12 myoblasts • stem cell therapy

Introduction

In recent years, the strategies for primary prevention of cardiovascular disease and the improvement of emergency therapeutic protocols have dramatically changed the clinical outcome of myocardial infarction, because an ever-increasing number of patients survive the acute phase of this disease. The other aspect of the medal consists in increased occurrence of long-term complications due to adverse myocardial remodelling, mainly impaired myocardial contractile function and heart failure [1]. In fact, the myocardium possesses scarce regenerative potential, being composed mainly of mature cardiomyocytes unable to self-renew. Despite the adult heart does contain muscle stem cells with the potential to proliferate and differentiate [2–4], these cells are actually incapable of regenerating the damaged

[†]M.B and S.N. contributed equally to this article.
*Correspondence to: Prof. Daniele BANI,
Department of Anatomy, Histology & Forensic Medicine,
University of Florence,
viale G.Pieraccini, 6
I-50139, Florence, Italy.
Tel.: +39-0554271390
Fax: +39-0554271385
E-mail: daniele.bani@unifi.it

doi:10.1111/j.1582-4934.2008.00503.x

myocardium and improving the clinical symptoms of heart failure [5]. Therefore, the attention of many researchers has been long-focused on extra-cardiac stem cells with the ability, at least in principle, to differentiate into the cardiac muscle phenotype [6]. In this context, stem cell grafting for cardiac repair is viewed as the new frontier in the treatment of post-infarction heart failure [7–9]. Skeletal myoblasts, for example, have been considered promising candidates [10], mainly because they are resistant to ischaemia and hence may survive within the poorly vascularized myocardial scar. Further, these cells can be isolated and expanded *ex vivo* from skeletal muscle biopsies of the same patients scheduled for cell grafting therapy, with obvious immunological and ethical advantages [6, 10]. Although engrafted skeletal myoblasts do not exhibit the potential to differentiate into myocardial-like cells [11], numerous studies have demonstrated a significant improvement of the heart's contractile performance upon myoblast transplantation [12, 13]. A possible explanation for this ostensible paradox has come from the results of recent experimental studies, suggesting that the grafted cells may release paracrine cardiotropic factors capable of inducing collagen remodelling and neoangiogenesis in the recipient hearts [14, 15].

Based on the above-reported observations, it appears that further investigations are needed to shed light on the mechanisms underlying the functional advantages of myoblast grafting in the post-ischaemic heart and to better define the possible therapeutic protocols. A novel approach may be the combination of myoblast cell grafting and cellular therapy, whereby cells can act as carriers for genes encoding cardiotropic substances that can be delivered locally [10]. Indeed, a recent study from our group showed that the cardiotropic hormone relaxin (RLX) is capable of improving the contractile performance of post-infarcted swine hearts by positively influencing cardiac remodelling and neo-angiogenesis [15]. RLX is a member of a peptide hormone family, which includes three distinct RLX molecules (denoted H1, H2 and H3, respectively), as well as insulin-like peptides (INSL) 3 to 6 [16, 17]. In human beings, three separate RLX genes have been found and designated *RLN1*, *RLN2* and *RLN3* [16, 17]. Relaxin-2 (H2), encoded by the *RLN2* gene, is the major circulating form and accounts for most of the known biological effects of RLX in human beings and experimental animals. RLX acts on both reproductive and non-reproductive tissues [17–22] and exerts major effects on the cardiovascular system [17, 21, 22]. Some of these effects, namely increased heart perfusion [23], neo-angiogenesis [24] and reduced cardiac fibrosis by increased extracellular matrix (ECM) turnover [25], are potentially relevant to cell grafting therapy. In fact, it may be speculated that H2 RLX could be employed, both as a drug and as a functional transgene, for cellular- or gene-based therapy of post-infarction cardiac disease.

Therefore, we designed the current study to determine whether skeletal myoblasts, wild-type or engineered to expressed RLX, and exogenously administered RLX are capable of improving the long-term sequelae in a rat model of chronic myocardial infarction and to investigate the possible mechanisms involved.

Materials and methods

Generation and culture of engineered C2C12 myoblast cell lines

Mouse skeletal C2C12 myoblasts (ATCC, Manassas, VA, USA) were cultured in DMEM containing 10% foetal bovine serum (Sigma, Milan, Italy). Cells were transduced with an integrating lentiviral vector bicistronically expressing human preprorelaxin 2 cDNA [26] and eGFP gene, or just eGFP, under a cytomegalovirus (CMV) promoter. These cell strains have been termed C2C12/RLX and C2C12/GFP, respectively. Day 2 supernatants from C2C12/RLX cell cultures contained 1.8 ± 0.2 ng/ml RLX, as assessed by a human H2 RLX-specific ELISA [15]. Clones were selected by cloning ring method and analysed by fluorescent microscopy and flow cytometry for eGFP expression. Cells were grown in DMEM, containing 10% foetal bovine serum (Sigma) and 0.1% gentamycin, in a 5% CO_2 atmosphere at 37°C. When required for transplantation, cells were detached using EDTA 0.1% in phosphate-buffered saline (PBS) and mechanical scraping, centrifuged and washed twice in PBS and finally re-suspended in complete culture medium, as described below. Cell concentration was determined using a Bürker chamber and adjusted to the amount required for individual injections.

Surgery and experimental protocols

The experimental protocol complied with the Declaration of Helsinki and the recommendations of the European Economic Community (86/609/CEE) on animal experimentation. Wistar male rats, weighing 250–300 g, under general anaesthesia and artificially ventilated, underwent ligation of the left anterior descending coronary artery after the first diagonal branch to induce myocardial infarction, as previously described [27]. The animals were then placed in cages under controlled temperature and high pO_2 to facilitate post-operative recovery until achievement of a normal respiratory activity and cardiac beating rate (350–450 beats/min.). Rats were housed under standard conditions until the next experimental step.

Thirty days after surgery, the animals were divided in four experimental groups.

Group 1 – Infarcted controls ($n = 5$). These rats were re-operated by the same procedure as above and a 24-gauge silicone catheter was placed in the *vena cardiaca magna* through the *vena cava superior* to deliver 1 ml of DMEM culture medium at a 1 ml/min. perfusion rate.

Group 2 – Infarcted, RLX-treated ($n = 5$). These rats were re-operated and catheterized as above to deliver DMEM alone. At the same time, mini-osmotic pumps (mod. 2004; Alzet, Cupertino, CA, USA), having a 0.25 μl/hr pumping rate and filled with 200 μl PBS containing 33 μg human recombinant H2 RLX (kindly provided by Dr Mario Bigazzi, Prosperius Institute, Florence, Italy), were implanted into the peritoneal cavity. These devices permitted the delivery (i.p.) of a daily RLX dose of 1 μg for 28 days.

Group 3 – Infarcted, C2C12/GFP-treated ($n = 5$). These rats were re-operated and catheterized to deliver C2C12/GFP myoblasts ($2 \cdot 10^6$ cells/100 g b.wt. in 1 ml DMEM).

Group 4 – Infarcted, C2C12/RLX+RLX-treated ($n = 8$). These rats were re-operated and catheterized to deliver C2C12/RLX myoblasts (2×10^6 cells/100 g b.wt. in 1 ml DMEM). Moreover, mini-osmotic pumps (mod. 2004, Alzet) releasing 1 μg/day human recombinant H2 RLX for 28 days were implanted into the peritoneal cavity, as in group 2.

To prevent reflow, in all animals, the *vena cardiaca magna* was tied to the infusion catheter for 10 min. In the previous studies used as reference for the design of the present experimental protocol, a 5-min. occlusion of the catheterized *vena cardiaca magna* allowed the settlement of about 30% of total grafted myoblasts within the heart, evaluated as soon as 10 min. after delivery [27, 28].

Following recovery, rats were housed under standard conditions for further 60 days. The animals of all groups underwent daily oral administration of cyclosporine (15 mg/kg b.wt.) to obtain immune suppression and enhance the success of C2C12 cell xenografting. Rat mortality upon the first intervention for induction of myocardial infarction was 20–30% and mortality upon re-operation ranged between 40% and 50%. The experiment was terminated when each group comprised at least five animals.

Circulating levels of RLX in groups 2 and 4 were measured 1 month (T2) and 2 months (T3) after osmotic pump implantation using a commercial human H2 RLX ELISA kit (Immundiagnostik, Bensheim, Germany). In the former case, animals were anaesthesized by isoflurane inhalation and 0.5 ml blood samples were collected by tail vein puncture and centrifuged at 500 *g* for 15 min. at 20°C to separate plasma. In the latter case, blood samples were taken from the superior *vena cava* before heart removal for tissue sampling.

Echocardiographic assessment of cardiac function

The animals of the four groups were anaesthesized and subjected to transthoracic bi-dimensional M-mode echocardiography using a Sequoia 512 device (Siemens Acuson, Erlangen, Germany) equipped with a 15-MHz probe to evaluate overall and segmental left ventricular dynamics and hence heart contractile performance [29, 30]. The following parameters were measured or calculated: (*i*) left ventricular end-diastolic diameter, LVEDD; (*ii*) left ventricular end-systolic diameter, LVESD; (*iii*) fractional shortening, FS; (*iv*) left ventricular ejection fraction, LVEF; (*v*) myocardial performance index, MPI, the sum of isovolumetric contraction and relaxation times/ejection time. This assay was carried out prior (T0) and 1 month after (T1) the induction of myocardial infarction, as well as 1 (T2) and 2 (T3) months after DMEM, RLX or cell delivery.

Micro-PET analysis of myocardial viability and performance

Positron emission tomography (PET) scans on the rats of the different groups were performed after administration of the viability tracer ^{18}fluorodeoxyglucose (^{18}F-FDG), as previously described [31, 32]. ^{18}F-FDG is taken up by metabolically active cells (*e.g.* the uninjured cardiomyocytes), thus allowing measurement of the volume of viable myocardium. Each animal was anaesthesized with 4% sevofluorane/oxygen, injected i.p. with glucose solution to standardize glucose and insulin levels and, 20 min. later, given 45 MBq ^{18}F-FDG, injected in the tail vein in a 0.15-ml volume. The residual dose in the syringe was measured to verify the effective dose injected. At the end of the uptake time (30 min.), PET image acquisition was performed with a GE eXplore Vista DR small-animal PET tomograph (GE Medical System, Paris, France) with the anaesthesized rat placed prone on the scanner bed (two bed positions, 15 min. each). Once the scan was completed, the animal was allowed to wake up in a warmed recovery cage. PET images of FDG-positive heart tissue areas were reconstructed iteratively with a 2-D ordered-subsets expectation maximization algorithm (OSEM 2-D) using a specific software (ECTB, Emory University, Atlanta, GA, USA). In this manner, myocardial metabolic function and its treatment- and time-related changes were semi-quantitatively evaluated. PET assay was carried out 1 month after the induction of myocardial infarction (T1), as well as 1 (T2) and 2 (T3) months after DMEM, RLX or cell delivery.

Cardiac tissue sampling and analysis

After the last functional assays at the T3 time-point, rats were killed by lethal i.p. penthotal injection. At autopsy, cardiac tissue samples were excised downstream the coronary occlusion, as well as from the non-ischaemic inter-ventricular septum, for morphological analyses. Unless otherwise stated, some tissue fragments were fixed in 3% paraformaldehyde in PBS, pH 7.4, dehydrated in graded ethanol and embedded in paraffin; other fragments were cryoprotected in sucrose 30% in PBS, washed in PBS and quickly frozen and stored at −80°C until use.

Immunofluorescence for detection of eGFP-expressing cells

Cryostat sections, 10 μm thick, were cut from frozen tissue samples, fixed in paraformaldehyde vapours for 10 min. and incubated with rhodamine-conjugated mouse monoclonal anti-eGFP (Santa Cruz, CA, USA; 1:200) to detect engineered C2C12 cells. Negative controls were performed with non-immune mouse serum substituted for the primary antibody. Cells were examined and photographed under a Zeiss Axioskop fluorescence microscope (Zeiss, Oberkochen, Germany). For optimal rendering, phase-contrast and immunofluorescent micrographs were taken from the same microscopic fields and then merged by a commercial image processing software.

Ultrastructure of cardiac tissue

Cardiac tissue samples were fixed in glutaraldehyde-osmium tetroxide, embedded in epoxy resin and routinely processed for transmission electron microscopical (TEM) observation. Other fragments, not osmium-fixed, were used for immuno-electron microscopy to detect RLX in the grafted C2C12/RLX cells. Ultra-thin sections were etched with 30% hydrogen peroxide and incubated with normal goat serum (Sigma; 1:20) to quench nonspecific binding sites, then with rabbit polyclonal anti-H2 RLX antibodies (Immundiagnostik; 10 μg/ml) and finally with goat anti-rabbit antibodies conjugated with 5 nm colloidal gold particles (BBInternational, Stanstead, UK; 1:20). Sections in which non-immune goat serum was substituted for the primary antiserum were used as negative controls. The sections were counterstained with uranyl acetate and lead citrate and examined under a Jeol 1010 (Jeol, Tokyo, Japan) electron microscope at 80 kV.

Determination of fibrosis

Fibrosis in the cardiac scar was studied by qualitative and quantitative morphological methods on paraformaldehyde-fixed, paraffin-embedded samples. Sections 7-μm were stained with a modified Azan method for connective tissue, in which azocarminium was omitted to reduce parenchymal tissue background. Five fields per animal were registered by a digitizing camera applied to a light microscope with a 25 x objective, each

field corresponding to a test area of 58,800 μm^2. On the digitized images, measurements of overall surface area (SA) and optical density (OD) of the anilin blue-stained collagen fibres were carried out using the free-share ImageJ 1.33 image analysis program (http://rsb.info.nih.gov/ij), upon appropriate threshold to exclude amorphous ground substance and unstained myocardium. For each animal, a sclerosis index was calculated by the formula: $SAxODx10^{-6}$. Values from the five animals in each group were then averaged.

Determination of microvessel density

Microvascular density (MVD) in the cardiac scar tissue was measured by point counting on 2−μm-thick semi-thin sections of resin-embedded samples, as described [15]. Ten microscopical fields (20 × objective) per animal were registered by the same device described above. A morphometric square grid (test area, 147,000 μm^2; 130 test points; 12-mm distance between line intersection points, corresponding to 30 μm on the image) was superimposed on each image. MVD was then calculated as the number of the points on transverse or slightly oblique microvessel profiles in each test area. Measurements performed by two independent observers were averaged.

Determination of cardiac cell apoptosis

Apoptosis detection was carried out by TUNEL assay on sections from formalin-fixed, paraffin-embedded samples using a FragEL™–Klenow DNA Fragmentation Detection Kit (Oncogene, San Diego, CA, USA) according to the manufacturer's instructions. Briefly, the sections were rehydrated in graded ethanol and incubated with 15 mg/ml proteinase K for 15 min. at room temperature. After rinsing in PBS, endogenous peroxidase was inactivated by incubating the sections in 3% H_2O_2 for 5 min. at room temperature. After a further PBS rinsing, the sections were immersed in terminal deoxynucleotidyltransferase (TdT) buffer containing deoxynucleotidyl transferase and biotinylated dUTP, incubated in a humid atmosphere at 37°C for 90 min., and then washed with PBS. Then, the sections were incubated at room temperature for 30 min. with peroxidase-conjugated streptavidin and the signal was revealed with 3,3′-diaminobenzidine. Finally, nuclear counterstaining was achieved by Methyl green. Apoptotic nuclei were recognized by the presence of dark brown staining, at variance with those of viable cells, which instead appeared pale brown or green. From each sample, 4 microscopic fields (40 × objective) were chosen at random from the myocardium close to the scar tissue. The overall number of cardiomyocyte nuclei was counted and the percentage of the positive ones was calculated. An average of 200 nuclei was counted for per each animal. Two observers carried out the measurements on the same microscopic fields and the individual values were then averaged.

Determination of cycling cardiac cells

Immunocytochemical detection of the nuclear antigen Ki-67 was performed on sections from formalin-fixed, paraffin-embedded samples. The sections were dewaxed in xylene, rehydrated in graded ethanol, treated with 2% H_2O_2 in methanol (v/v) for 2 min. to quench endogenous peroxidase, then warmed for 5 min. in citrate buffer in a microwave oven to retrieve antigens and finally incubated with mouse monoclonal anti-Ki-67 antiserum (MIB-1 clone, Dako, Milan, Italy; 1:50 in PBS) overnight at 4°C. Immune reaction was revealed by indirect immunoperoxidase method (Vectastain Elite kit, Vector, Burlingame, CA, USA), using 3,3′-diaminobenzidine as the chromogen. In the negative controls, PBS was substituted for the primary antiserum. Nuclear counterstaining was done by haematoxylin.

Statistical analysis

Values are means ± S.E.M. of the animals in each group. Differences between the experimental groups were evaluated by one-way ANOVA and Newman–Keuls post-test. Calculations were made with Prism 4 (GraphPad, San Diego, CA, USA) statistical program.

Results

Echocardiography

In all the animals, surgical induction of myocardial infarction caused a marked decay of the assayed echocardiographic parameters of cardiac function. Namely, 1 month after surgery (T1), LVEF and FS were significantly reduced, whereas LVEDD, LVESD and MPI were significantly increased in comparison with the pre-operative (T0) values (Fig. 1). In the untreated controls (group 1), these parameters remained substantially unchanged in the successive measurements carried out 1 month (T2) and 2 months (T3) after re-operation, at variance with significant improvements in the rats subjected to the therapeutic treatments. In particular, (*i*) LVEF was significantly increased in the rats which received C2C12/GFP (group 3) and even more in those which received C2C12/RLX+RLX (group 4); (*ii*) FS was significantly increased in the rats given both RLX alone (group 2) and C2C12/RLX+RLX (group 4) at T2, and in all the treated animal groups at T3: at both time-points, the best performance was achieved by the rats of group 4; (*iii*) LVEDD and LVESD were significantly reduced in all the treated animal groups at T2 and even more at T3; LVEDD was similarly improved in all the three groups, whereas LVESD was particularly reduced in the animals receiving C2C12 engraftment; (*iv*) MPI were significantly and similarly reduced in all the treated animal groups at T2 and even more at T3.

Micro-PET analysis

Quantitative tomographic analysis of cardiac ^{18}F-FDG uptake showed that, 1 month after surgical induction of myocardial infarction (T1), the rats of all the experimental groups had a marked reduction of the overall volume of viable myocardium (Fig. 2). In many cases, this viability defect, appearing as a hypo-metabolic, radio-negative region, involved the antero-septal

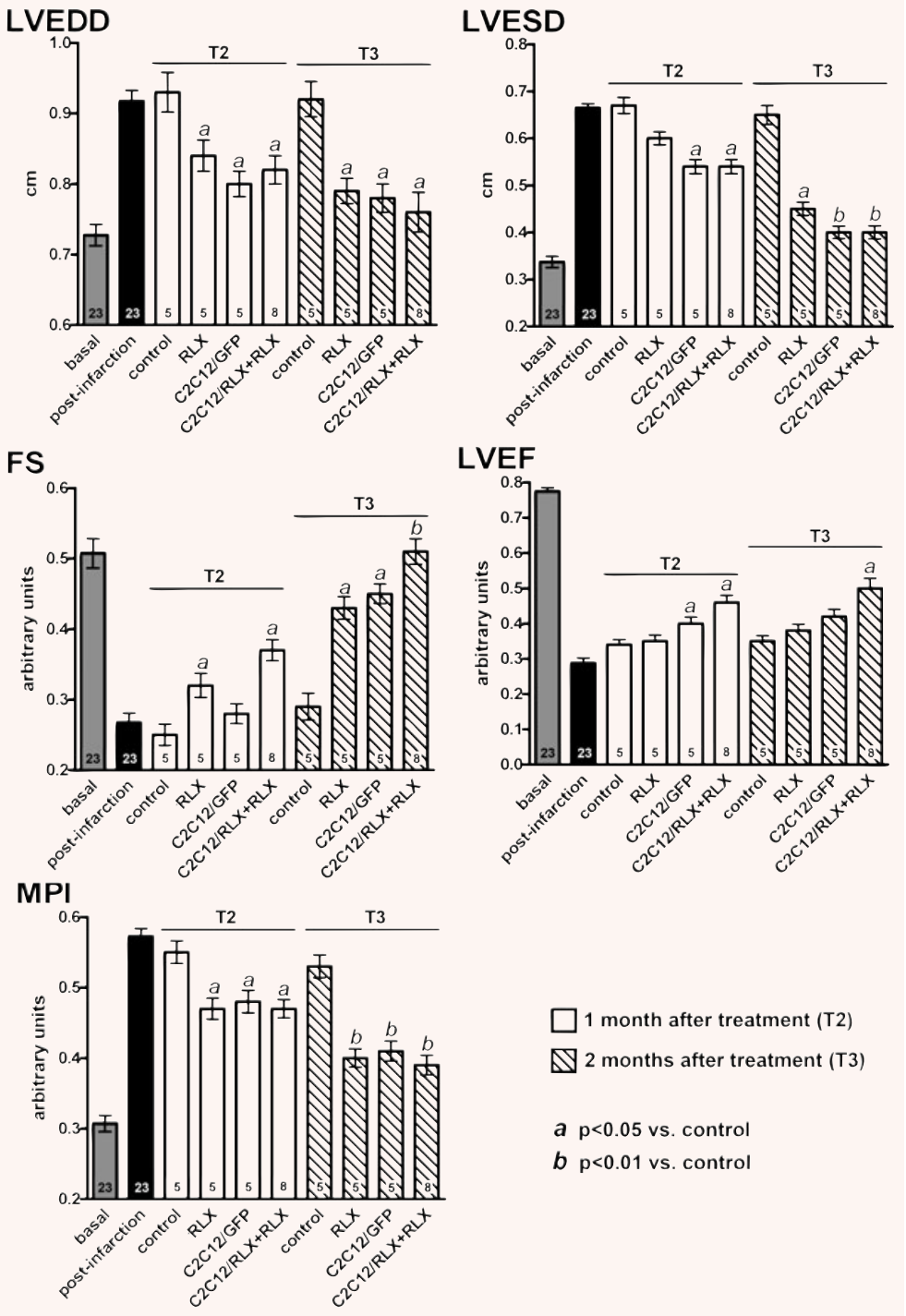

Fig. 1 Echocardiographic parameters of cardiac function at different time-points: basal pre-operative values (T0, grey columns), 1 month after surgical induction of myocardial infarction (T1, black columns), 1 month (T2, open columns) and 2 months (T3, striped columns) after the therapeutic treatments. FS, fractional shortening; LVEDD, left ventricular end-diastolic diameter; LVESD, left ventricular end-systolic diameter; LVEF, left ventricular ejection fraction; MPI, myocardial performance index. The number of rats per group is reported at the bottom of each column.

left ventricular wall and was substantially similar in all the animals examined. Treatment with C2C12/RLX+RLX induced a clear-cut, statistically significant increase ($P < 0.01$) in the volume of viable myocardium as early as 1 month after cell grafting (T2) and even more at 2 months (T3), accounting for an increase of 16% and 31%, respectively, over the values measured at T1. On the other hand, treatment with C2C112/GFP only significantly increased the viability of the myocardium at T3 ($P < 0.05$), whereas RLX alone had little or no effect on this parameter.

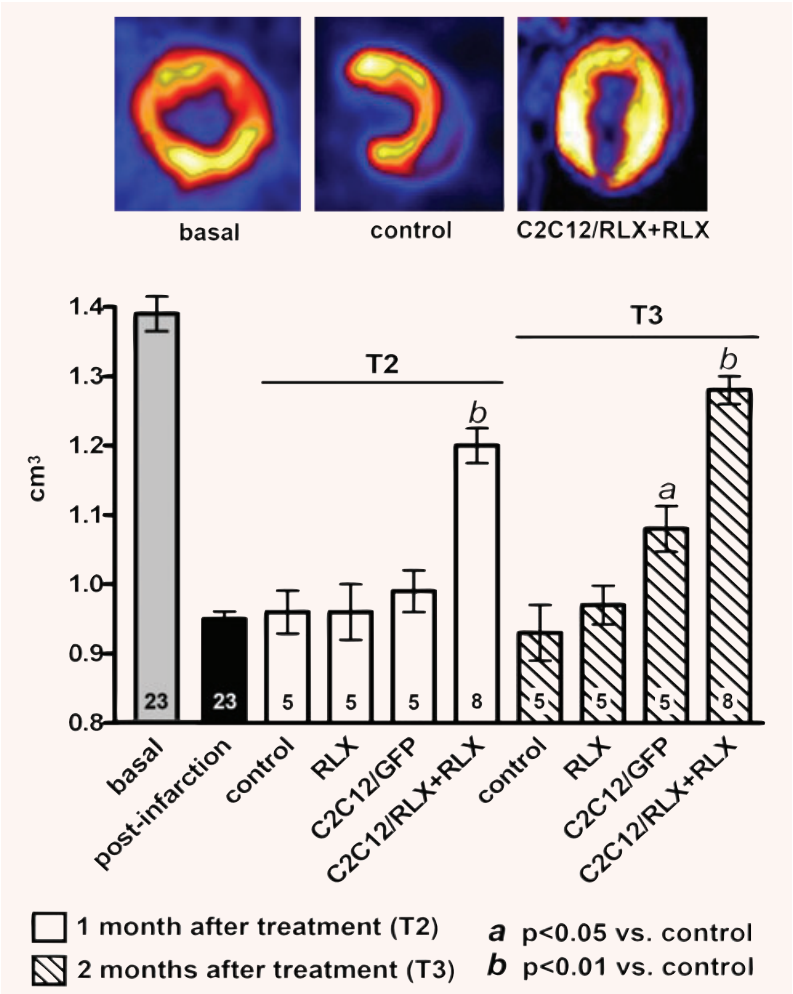

Fig. 2 Myocardial viability evaluated by micro-PET analysis. Upper panels: representative images of cardiac ^{18}F-FDG uptake from post-infarcted rats given culture medium alone (control) or C2C12/RLX+RLX. A large uptake defect of the viability tracer by the ventricular myocardium can be seen in the control, but not in the treated heart. Lower panel: overall viable ventricular volume measured 1 month after surgical induction of myocardial infarction (T1, black columns), 1 month (T2, open columns) and 2 months (T3, striped columns) after the therapeutic treatments. The number of rats per group is reported at the bottom of each column.

Localization of the grafted cells in the host hearts

Relatively few immunoreactive eGFP-expressing C2C12 were found in the scar tissue from groups 3 and 4 (Fig. 3A and B). By visual observation, the hearts of C2C12/GFP-treated animals contained lower amounts of immunoreactive cells compared with those treated with C2C12/RLX+RLX. The engrafted cells were mainly located in the proximity of blood vessels, whereas they were not detected in the viable myocardium not involved in post-infarction remodelling. Immuno-electron microscopy of cardiac scar specimens from rats transplanted with C2C12/RLX cells revealed the occurrence of RLX-producing cells, identified by the presence of RLX immuno-gold labelling on cytoplasmic areas occupied by organelles involved in protein synthesis and secretion, *i.e.* RER and Golgi cisternae (Fig. 3C). As expected, RLX-immunoreactive cells were not found in the hearts transplanted with C2C12/GFP (data not shown). The engrafted myoblasts could be distinguished by the activated fibroblasts in the scar because they never showed any signs of collagen secretion and fibre build-up, as those described forward. Of note, none of the C2C12 cells encountered showed any tendency to fuse into multinucleated myotubes or to develop myofibrils, thus suggesting that they are unable to regenerate contractile tissue at the grafting site, at least under the current experimental conditions.

Histological features of post-infarcted hearts

By modified Azan staining (Fig. 4, upper panels), the post-infarction cardiac scar from the untreated control animals showed densely packed bundles of collagen fibres. Conversely, samples from rats subjected to the therapeutic treatments (groups 2 to 4) exhibited a reduction in the amount of collagen fibres, confirmed by morphometric analysis of tissue collagen content expressed as sclerosis index (Fig. 4, centre panel). By TEM (Fig. 4, lower panels), fibroblasts in the tissue samples from the untreated controls

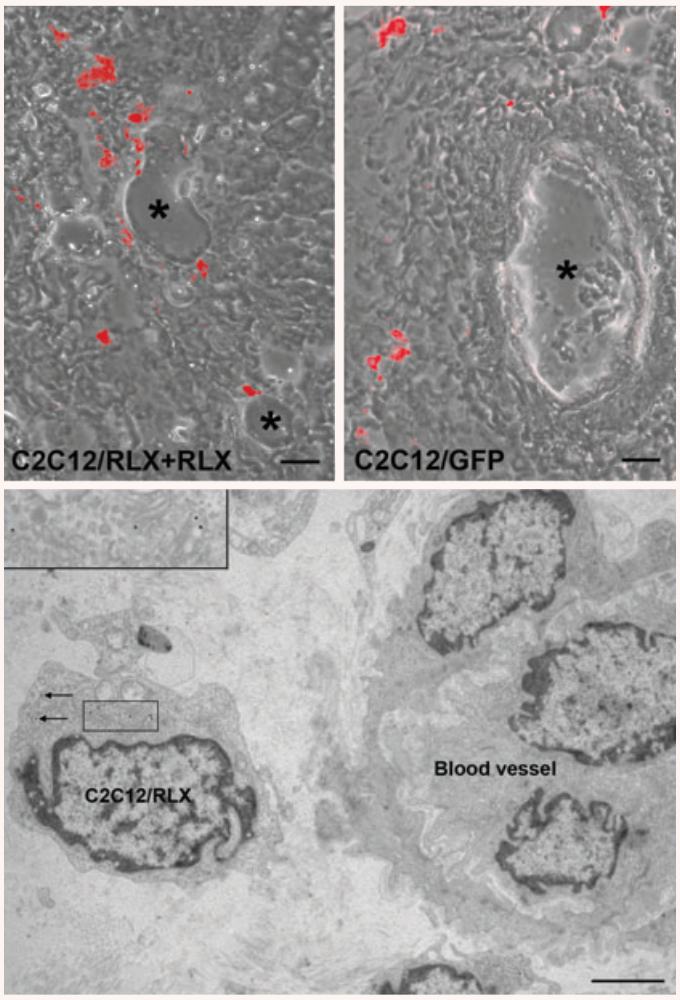

Fig. 3 Upper panels: representative micrographs of C2C12/GFP and C2C12/RLX myoblasts grafted in the post-infarction cardiac scar, immunostained to reveal eGFP. The asterisks label blood vessel lumina. Merged phase contrast and immunofluorescent images. Bars = 20 μm. Lower panel: representative electron micrograph showing a C2C12/RLX in close proximity of a microvessel, immunolabelled to reveal RLX by 10-nm gold particles (arrows and inset). The particles are located on RER and Golgi profiles. Bar = 1 μm.

appeared as activated cells: their cytoplasms contained abundant RER and large Golgi complexes and their plasma membranes were characterized by sites of apposition to thin electron-dense filaments, featuring collagen microfibrils undergoing pericellular processing and assembly. Moreover, large collagen bundles were present in the ECM. In rats receiving C2C12/RLX+RLX, as well as in those treated with H2 RLX alone, fibroblasts featured predominantly quiescent cells, with no evidence of pericellular collagen microfibril assembly, and were immersed in a loose, electron-lucent ECM with few, thin collagen fibrils. In contrast, the samples from rats receiving C2C12/GFP showed ultrastructural features not substantially different from those of the untreated controls.

To explore the effects of RLX on scar tissue vascularization and angiogenesis, microvascular density (MVD) was measured. Sections of cardiac tissue harvested from rats of groups 2, 3 and 4 exhibited a significant increase in MVD compared to the untreated controls of group 1. No significant differences were observed between the therapeutic treatments (Fig. 5).

Determination of apoptotic and proliferating cardiac cells

To provide further insight into the mechanisms of the observed improvement of the post-infarcted hearts subsequent to therapeutic treatments, we examined and quantified the amount of apoptotic and cycling cells in the myocardium surrounding the scar. By TUNEL assay (Fig. 6), the untreated controls showed a relatively large amount of apoptotic cardiomyocytes. Apoptotic cells were significantly reduced in the hearts from rats subjected to the therapeutic treatments, especially those of groups 2 and 4. By Ki-67 immunocytochemistry, very few positive cycling cells were encountered: they were mostly isolated cells of the scar tissue or sparse endothelial cells of microvessels in the scar or the border-line myocardium (data not shown). No differences were observed between the different experimental groups.

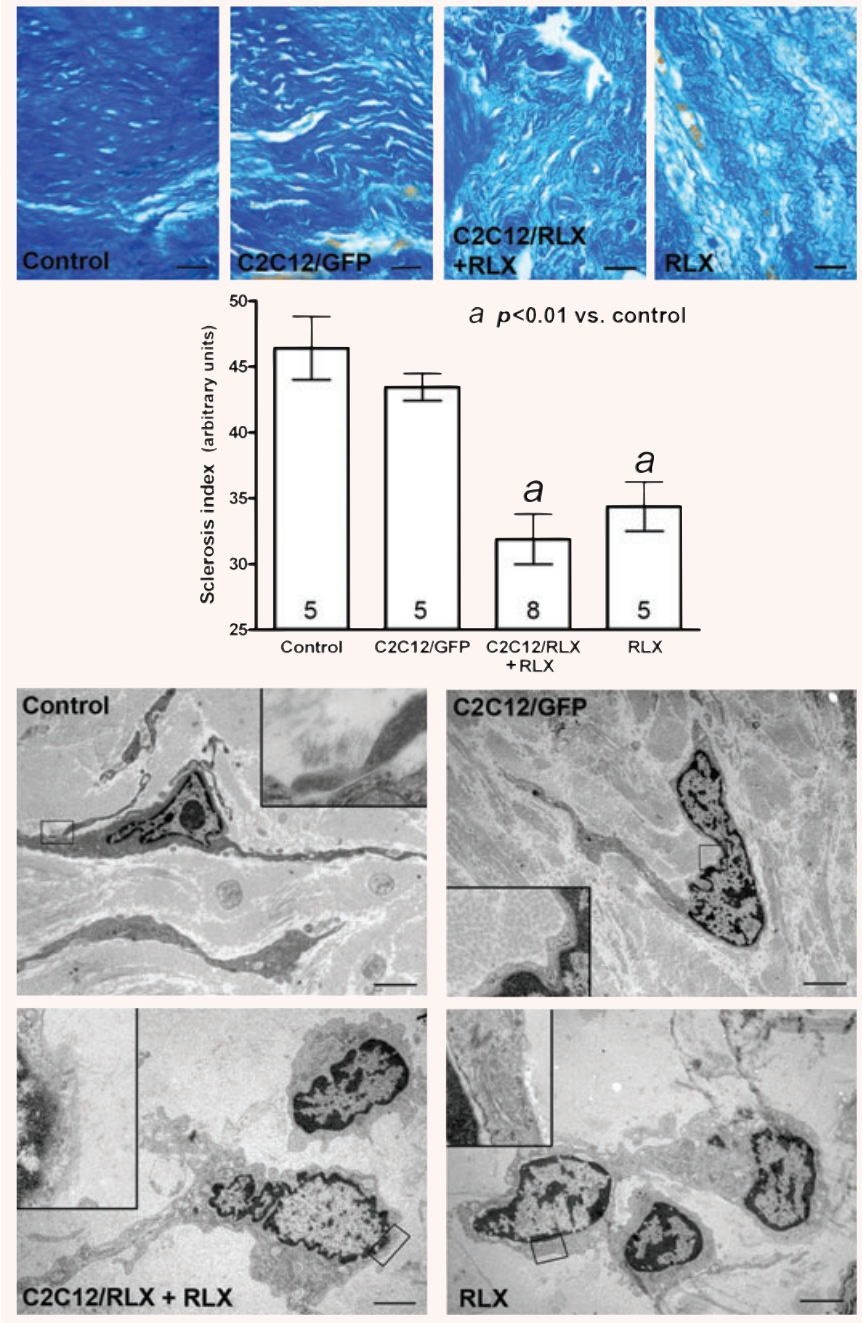

Fig. 4 Upper panels: representative micrographs of anilin blue-stained sections of post-infarction cardiac scar from the different animal groups. Bars = 10 μm. Centre panel: morphometric analysis of scar tissue collagen content, expressed as sclerosis index (surface area · optical density/10^6) in the different experimental groups. The number of rats per group is reported at the bottom of each column. Lower panels: representative electron micrographs showing fibroblasts (note the extended RER and Golgi apparatus) and the surrounding ECM (with varying amounts of collagen fibres) in the different experimental groups. The insets show sites of apposition of the cell's plasma membrane to thin electron-dense filaments, which feature assembling collagen microfibrils. The inset to the lower right micrograph is a detail of the Golgi area. Bar = 1 μm.

Plasma RLX levels

One month after the therapeutic treatments (T2), in the rats treated with C2C12/RLX+RLX and H2 RLX alone, plasma RLX levels were 82 ± 37 and 75 ± 29 ng/ml, respectively. Two months after the treatments (T3), RLX plasma concentration fell below the sensitivity of the assay. As expected, RLX levels were undetectable in all samples from untransplanted controls and C2C12/GFP-treated animals.

Discussion

Using a rat model of chronic myocardial infarction suitable for long-term investigation of heart remodelling, we performed a detailed functional analysis by combining echocardiographic assessment of cardiac performance and PET-based metabolic imaging of myocardial viability. This approach allowed us to achieve a careful time-course evaluation of cardiac failure and of

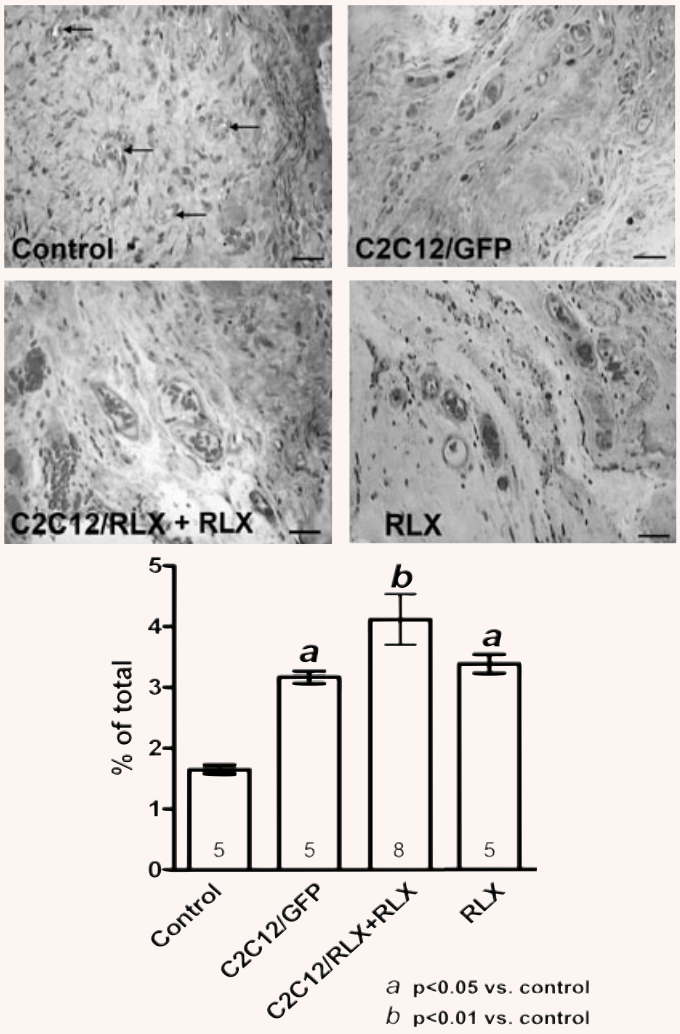

Fig. 5 Upper panels: representative micrographs of semi-thin sections of post-infarction cardiac scar from the different animal groups showing varying numbers of microvascular profiles. Bars = 10 μm. Lower panel: morphometric analysis of the relative volume density of microvessels (MVD) over the total scar tissue in the different groups. The number of rats per group is reported at the bottom of each column.

the benefits afforded by the different therapeutic treatments. Taken together, the results of the functional and histopathological analyses provide further experimental evidence that stem cell grafting can improve myocardial performance and survival during post-infarction heart remodelling and offer background to the novel concept that genetically manipulated grafted cells can effectively be used for local delivery of therapeutic cardiotropic molecules [10, 33, 34]. The current findings also indicate that RLX can be an effective agent in protecting the post-infarcted heart from adverse remodelling, in keeping with the emerging concept that this hormone, due to its collagen-remodelling, pro-angiogenic and vasodilatatory properties [23–25], can play a major cardioprotective role [17, 21, 22, 34].

This study confirms and extends our previous findings obtained by transplantation of RLX-producing C2C12 cells in post-infarcted swine, examined 1 month after cell injection [15]. The current rat experimental model provides similar evidence that improved ECM turnover and neo-angiogenesis are a prominent feature of the functional benefits afforded by C2C12 cells and RLX, even upon long-term cardiac remodelling (2 months): moreover, it first indicates that selective homing of grafted myoblasts to the post-infarction scar tissue in combination with local/circulating RLX result in enhanced survival of peri-lesional myocardium.

The combination of C2C12/RLX cells, which secrete RLX at the sites of cell engraftment, and osmotic pumps releasing exogenous RLX appears to offer synergistic advantages. Exogenous RLX alone, although promoting the improvement of some echocardiographic (FS, LVEDD and MPI) and histopathological (sclerosis index and microvascular density) parameters, had little or no effects on residual myocardial viability, as assessed by micro-PET. These findings suggest that systemic RLX administration chiefly influences cardiac remodelling towards a less stiffened cardiac

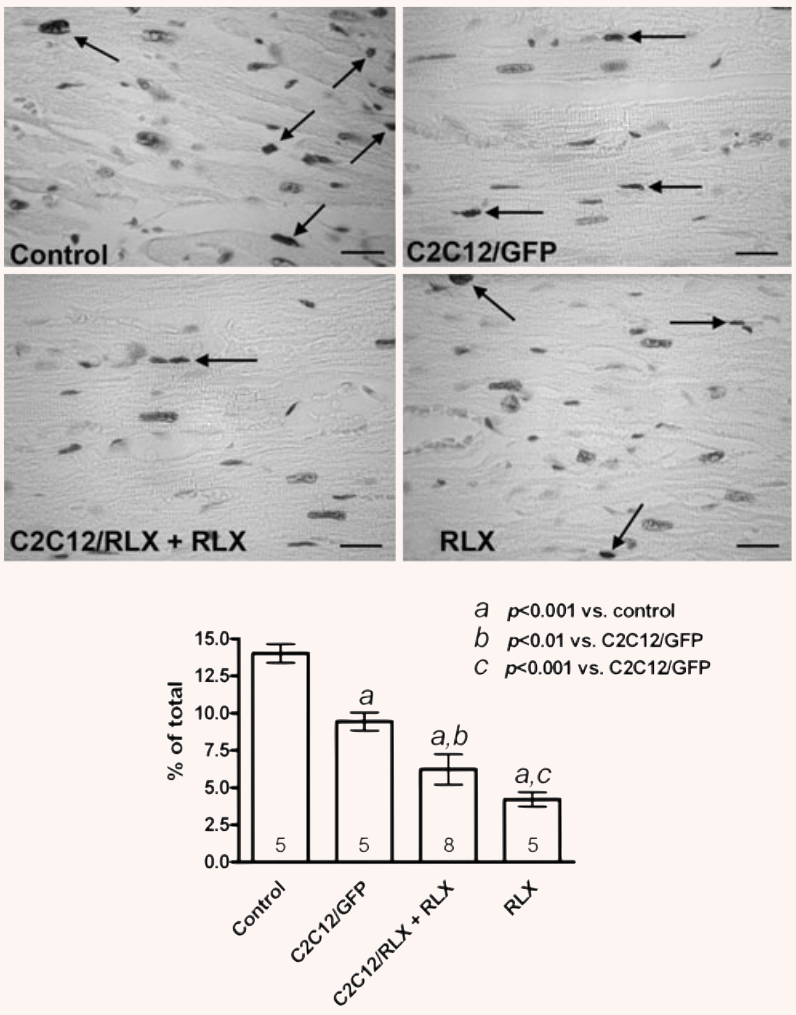

Fig. 6 Upper panels: representative micrographs of histological sections of the myocardium surrounding the cardiac scar taken from the different animal groups subjected to TUNEL assay for apoptotic cells. The dark-stained, positive cardiomyocyte nuclei are indicated by arrows. Bars = 10 μm. Lower panel: morphometric analysis of the percentage of positive nuclei over the total ones in the different groups. The number of rats per group is reported at the bottom of each column.

scar [17], thereby improving diastolic compliance and ventricular contractile dynamics. When exogenous RLX was combined with grafting of C2C12/RLX cells, we observed a further beneficial effect, consistent with a statistically significant increase in the overall volume of viable myocardium. This effect appears to depend, at least in part, to the protection against myocardial cell apoptosis. Interestingly, this fits well with the recent observation that RLX antagonizes apoptosis in cultured rat cardiomyocytes [35]. Considering the effects of exogenously given RLX observed in animal models of acute myocardial infarction [36, 37], we suggest that local secretion of RLX by C2C12/RLX cells could exert paracrine effects on cardiac host tissue, favouring tissue perfusion and reducing local inflammation and sclerosis. By these mechanisms, RLX may promote survival and functional recovery of the stunned, peri-necrotic myocardium. It is even possible that, besides RLX, C2C12 cells could locally release other cardiotropic substances, as suggested by the observation that transplantation of C2C12/GFP also increases myocardial viability and cardiac functional performance. In fact, stem cells have been reported to release pro-survival and pro-angiogenic molecules when engrafted in the post-ischaemic heart [38, 39]. This is consistent with the recent 'paracrine' hypothesis to explain the functional benefits of stem cell therapy in the post-infarcted, dysfunctional heart [14, 15, 33, 34, 40].

The current findings also indicate that the retrograde coronary venous route for cell delivery is safe, as the mortality upon re-operation was similar in the treated and untreated animals, and adequate for the injected C2C12 cells to engraft into the host myocardium, where they could survive for at least 2 months after delivery. The relatively higher amounts of C2C12/RLX cells found at termination in the post-infarction scar as compared with C2C12/GFP cells suggest that RLX may

promote cell proliferation or, most likely, may favour cell engraftment and/or survival by re-modelling and improving the hostile milieu of the scar tissue [34]. Interestingly, C2C12 cells were localized mainly in the perivascular space, where they retain their original features of poorly differentiated precursors with no morphological sign of muscle-like differentiation. The inability of the C2C12 myoblasts to execute a myogenic differentiation programme in the cardiac scar has been previously highlighted in a similar study in the swine *in vivo* [15] and can be conceivably explained by the lack of appropriate micro-environmental signals in a non-physiological host tissue [41]. This finding offers additional support to the concept that transplanted myoblasts can improve the function of post-infarcted heart by indirect mechanisms, independent of *de novo* regeneration of contractile tissue [7, 8, 14, 34], and that RLX may be a candidate therapeutic to enhance efficacy of recovery.

From a practical point of view, the present study further underscores the therapeutic value of stem cell transplantation in post-infarction cardiac dysfunction, especially when the grafted cells are used as vehicle for the local release of cardiotropic substances capable of improving adverse heart remodelling [42]. The current findings also point to the option of using delayed rather than immediate cell therapy following acute myocardial infarction to achieve better efficacy, in keeping with previous reports [43].

Acknowledgements

The authors gratefully acknowledge Prof. Mario Bigazzi, Prosperius Institute, Florence, Italy, for the kind gift of human recombinant RLX. Many thanks are also due to Mrs. Laura Calosi, Mr. Daniele Guasti and Mrs. Rita Scantimburgo for skilful technical and administrative support.

References

1. **Jaber WA, Holmes DR Jr**. Outcome and quality of care of patients who have acute myocardial infarction. *Med Clin North Am.* 2007; 91: 751–68.
2. **Anversa P, Kajstura J.** Ventricular myocytes are not terminally differentiated in the adult mammalian heart. *Circ Res.* 1998; 83: 1–14.
3. **Messina E, De Angelis L, Frati G, *et al.*** Isolation and expansion of adult cardiac stem cells from human and murine heart. *Circ Res.* 2004; 95: 911–21.
4. **Bearzi C, Rota M, Hosoda T, *et al.*** Human cardiac stem cells. *Proc Natl Acad Sci USA.* 2007; 104: 14068–73.
5. **Torella D, Ellison GM, Méndez-Ferrer S, *et al.*** Resident human cardiac stem cells: role in cardiac cellular homeostasis and potential for myocardial regeneration. *Nat Clin Pract Cardiovasc Med.* 2006; 3: S8–13.
6. **Müller P, Beltrami AP, Cesselli D, *et al.*** Myocardial regeneration by endogenous adult progenitor cells. *J Mol Cell Cardiol.* 2005; 39: 377–87.
7. **Rubart R, Field LJ.** Cardiac regeneration: repopulating the heart. *Annu Rev Physiol.* 2006; 68: 29–49.
8. **Rubart R, Field LJ.** Stem cell differentiation: cardiac repair. *Cell Tiss Organs.* 2008; 188: 202–11.
9. **Vacanti CA.** The history of tissue engineering. *J Cell Mol Med.* 2006; 10: 569–76.
10. **Ye L, Haider HK, Sim EKW.** Adult stem cells for cardiac repair: a choice between skeletal myoblasts and bone marrow stem cells. *Exp Biol Med.* 2006; 231: 8–19.
11. **Reinecke H, Poppa V, Murry CE.** Skeletal muscle stem cells do not transdifferentiate into cardiomyocytes after cardiac grafting. *J Mol Cell Cardiol.* 2002; 34: 241–9.
12. **Taylor DA, Atkins BZ, Hungspreugs P, *et al.*** Regenerating functional myocardium: improved performance after skeletal myoblast transplantation. *Nat Med.* 1998; 4: 929–33.
13. **Rajnoch C, Chachques JC, Berrebi A, *et al.*** Cellular therapy reverses myocardial dysfunction. *J Thorac Cardiovasc Surg.* 2001; 121: 871–8.
14. **Caplice NM.** The future of cell therapy for acute myocardial infarction. *Nat Clin Pract Cardiovasc Med.* 2006; 3: S129–32.
15. **Formigli L, Perna AM, Meacci E, *et al.*** Paracrine effects of transplanted myoblasts and relaxin on post-infarction heart remodeling. *J Cell Mol Med.* 2007; 11: 1087–110.
16. **Bathgate RA, Samuel CS, Burazin TC, *et al.*** Relaxin: new peptides, receptors and novel actions. *Trends Endocrinol Metab.* 2003; 14: 207–13.
17. **Samuel CS, Du XJ, Bathgate RAD, *et al.*** 'Relaxin' the stiffened heart and arteries: the therapeutic potential for relaxin in the treatment of cardiovascular disease. *Pharm Ther.* 2006; 112: 529–52.
18. **Bani D.** Relaxin, a pleiotropic hormone. *Gen Pharmacol.* 1997; 28: 13–22.
19. **Conrad KP, Novak J.** Emerging role of relaxin in renal and cardiovascular function. *Am J Physiol Regul Integr Comp Physiol.* 2004; 287: 250–61.
20. **Sherwood OD.** Relaxin's physiological roles and other diverse actions. *Endocr Rev.* 2004; 25: 205–34.
21. **Dschietzig T, Bartsch C, Baumann G, *et al.*** Relaxin – a pleiotropic hormone and its emerging role for experimental and clinical therapeutics. *Pharm Ther.* 2006; 112: 38–56.
22. **Nistri S, Bigazzi M, Bani D**. Relaxin as a cardiovascular hormone. Physiology, pathophysiology and therapeutic promises. *Cardiovasc Hematol Agents Med Chem.* 2007; 5: 101–8.
23. **Bani Sacchi T, Bigazzi M, Bani D, *et al.*** Relaxin-induced increased coronary flow through stimulation of nitric oxide production. *Br J Pharmacol.* 1995; 116: 1589–94.
24. **Unemori EN, Lewis M, Constant J, *et al.*** Relaxin induces vascular endothelial growth factor expression and angiogenesis selectively at wound sites. *Wound Repair Regen.* 2000; 8: 361–70.
25. **Samuel CS, Unemori EN, Mookerjee I, *et al.*** Relaxin modulates cardiac fibroblast proliferation, differentiation, and collagen production and reverses cardiac fibrosis *in vivo*. *Endocrinology.* 2004; 145: 4125–33.
26. **Silvertown JD, Ng J, Sato T, *et al.*** H2 relaxin overexpression increases *in vivo* prostate xenograft tumor growth and angiogenesis. *Int J Cancer.* 2006; 118: 62–73.
27. **Suzuki K, Murtuza B, Fukushima S, *et al.*** Targeted cell delivery into infarcted rat hearts by retrograde intracoronary infusion: distribution, dynamics and influence on cardiac function. *Circulation.* 2004; 110: II-225–30.
28. **Suzuki K, Murtuza B, Smolenski RT, *et al.*** Selective cell dissemination into the heart by retrograde intracoronary infusion in the rat. *Transplantation.* 2004; 77: 757–9.

29. **Prunier F, Gaertner R, Louedec L, *et al.*** Doppler echocardiographic estimation of left ventricular end-diastolic pressure after MI in rats. *Am J Physiol Heart Circ Physiol.* 2002; 283: h346–52.
30. **Morgan EE, Faulx MD, McElfresh TA, *et al.*** Validation of echocaridiographic methods for assessing left ventricular dysfunction in rats with myocardial infarction. *Am J Physiol Heart Circ Physiol.* 2004; 287: h2049–53.
31. **Stegger L, Hoffmeier AN, Schäfers KP, *et al.*** Accurate noninvasive measurement of infarct size in mice with high-resolution PET. *J Nucl Med.* 2006; 47: 1837–44.
32. **Nanni C, Rubello D, Fanti S.** Role of small animal PET for molecular imaging in preclinical studies. *Eur J Nucl Med Mol Imaging.* 2007; 34: 1819–22.
33. **Gnecchi M, He H, Liang OD, *et al.*** Paracrine action accounts for marked protection of ischemic heart by Akt-modified mesenchymal stem cells. *Nat Med.* 2005; 11: 367–8.
34. **Du XJ.** Re-modelling 'hostile' milieu of diseased myocardium *via* paracrine function of transplanted cells or relaxin. *J Cell Mol Med.* 2007; 11: 1101–4.
35. **Moore XL, Tan SL, Lo CY, *et al.*** Relaxin antagonizes hypertrophy and apoptosis in neonatal rat cardiomyocytes. *Endocrinology.* 2007; 148: 1582–9.
36. **Bani D, Masini E, Bello MG, *et al.*** Relaxin protects against myocardial injury caused by ischemia and reperfusion in rat heart. *Am J Pathol.* 1998; 152: 1367–76.
37. **Perna AM, Masini E, Nistri S, *et al.*** Novel drug development opportunity for relaxin in acute myocardial infarction. evidences from a swine model. *FASEB J.* 2005; 19: 1525–7.
38. **Hu X, Yu SP, Fraser JL, *et al.*** Transplantation of hypoxia-preconditioned mesenchymal stem cells improves infarcted heart function *via* enhanced survival of implanted cells and angiogenesis. *J Thorac Cardiovasc Surg.* 2008; 135: 799–808.
39. **Unlu Y, Karapolat S.** Effects of implantation of bone marrow cells on cytokine levels in the ischemic heart tissue. An experimental study. *J Cardiothorac Surg.* 2008; 3: 30.
40. **Berry MF, Engler AJ, Woo YJ, *et al.*** Mesenchymal stem cell injection after myocardial infarction improves myocardial compliance. *Am J Physiol Heart Circ Physiol.* 2006; 290: H2196–203.
41. **Holterman CE, Rudnicki MA.** Molecular regulation of satellite cell function. *Semin Cell Dev Biol.* 2005; 16: 575–84.
42. **Haider HK, Ye L, Jiang SJ, *et al.*** Angiomyogenesis for cardiac repair using human myoblasts as carriers of human vascular endothelial growth factor. *J Mol Med.* 2004; 82: 539–49.
43. **Strauer BE, Brehm M, Zeus T, *et al.*** Regeneration of human infarcted heart muscle by intracoronary autologous bone marrow cell transplantation in chronic coronary artery disease: the IACT Study. *J Am Coll Cardiol.* 2005; 46: 1651–8.